

for the t' integration is released to $-\infty$. The error caused by these procedures is estimated to be bounded by the order $eE\gamma/q_c\epsilon_c$ and is negligible. On the other hand, the current expression is convergent without the restriction.

¹⁶Equation (11) can be obtained from Eq. (15) in Ref. 9(c) apart from a factor of 2 caused by the difference between β and β' , if we assume $\epsilon_c \ll k_B T$, as is the case for ordinarily dirty materials. In this case, the Bose character assumed by Masket *et al.* makes no effects. Although when $\epsilon_c \gg k_B T$ (which may occur in the case of extremely dirty materials), the assumed Bose character leads to Eq. (16) in Ref. 9(c), we will not make this assumption; therefore, Eq. (11) is correct in both cases.

¹⁷The magnitude of the value of ϵ_0' in Ref. 9(c) is half that of the present value. The factor of 2 in our expression is due to the use of β' instead of β .

¹⁸ R_N^{qs} and $\xi(0)$ are given in Table I, and $T_c = 1.9191$ K. The quantity $\alpha(0)$ is determined by $\alpha(0) = \hbar^2/2m\xi^2(0)$, and γ by $\gamma = \pi\alpha(0)/8k_B T_c$. To determine β we use $\beta = 1.02\hbar^2/nl^2m$ where $n = 5.56 \times 10^{22} \text{ cm}^{-3}$ and $l = 32 \text{ \AA}$ (Ref. 25). α_0' can be obtained from Eq. (7) with the above-mentioned values of T_c and γ , and α from Eq. (10) with the values of α_0' and β . This value of α is in plausible agreement with the value obtained by $\alpha = -\alpha(0)\epsilon = 7.3 \times 10^{-2} \text{ erg}$.

¹⁹See, for instance, H. L. Caswell, *J. Appl. Phys.* **32**, 105 (1961).

²⁰E. Abrahams, R. E. Prange, and M. J. Stephen, in Ref. 6; see also B. Serin, R. O. Smith, and T. Mizusaki, *ibid.* One of the authors (K. K.) is grateful to Dr. T. Mizusaki for his informative discussion on

this point.

²¹K. Maki, *J. Low-Temp. Phys.* **1**, 513 (1969).

²²K. Maki, *Progr. Theoret. Phys. (Kyoto)* **40**, 193 (1968); see also R. S. Thompson, *Phys. Rev. B* **1**, 327 (1970).

²³See, for instance, F. E. Harper and M. Tinkham, *Phys. Rev.* **172**, 441 (1968).

²⁴L. P. Gor'kov, *Zh. Eksperim. i Teor. Fiz.* **37**, 1407 (1959) [*Sov. Phys. JETP* **10**, 998 (1960)]; D. Saint-James, G. Sarma, and E. J. Thomas, *Type II Superconductivity* (Pergamon, New York, 1969), p. 151.

²⁵For the BCS coherence length ξ_0 , we used the relation $\xi_0 = 16000 T_{cb}/T_c (\text{\AA})$, where T_{cb} is the transition temperature of pure bulk aluminum, 1.175 K. See S. Caplan and G. Chanin, *Phys. Rev.* **138**, A1428 (1965).

²⁶For the experimental determination of T_c , see K. Kajimura and N. Mikoshiba, *J. Low-Temp. Phys.* **4**, 331 (1971).

²⁷K. Kajimura and N. Mikoshiba, *J. Low-Temp. Phys.* (to be published).

²⁸D. E. McCumber and B. I. Halperin, *Phys. Rev. B* **1**, 1054 (1970).

²⁹A. Kawabata, *Progr. Theoret. Phys. (Kyoto)* **45**, 365 (1971).

³⁰J. S. Langer and V. Ambegaokar, *Phys. Rev.* **164**, 498 (1967).

³¹A. Schmid, *Z. Physik* **231**, 324 (1970).

³²L. P. Gor'kov and G. M. Eliashberg, *Zh. Eksperim. i Teor. Fiz.* **54**, 612 (1968) [*Sov. Phys. JETP* **27**, 328 (1968)].

³³K. Maki, *Progr. Theoret. Phys. (Kyoto)* (to be published).

Antiferromagnetic Solution of the Hubbard Model*

Tadashi Arai†

Argonne National Laboratory, Argonne, Illinois 60439

and

Istituto di Fisica, Università di Messina, Messina, Italy

(Received 8 February 1971)

The Hubbard Hamiltonian for the system of one-electron atoms is solved in the presence of sublattice magnetization. In the limit of the fully antiferromagnetic state, the results reproduce those of Slater's split-band model by splitting a nonmagnetic band into spin-polarized bands. As magnetization decreases, antipolarized split bands appear and increase their strengths while the band gap remains constant. In the limit of no sublattice magnetization, the strengths of the two types of bands become equal, yielding the Hubbard nonmagnetic insulating state.

I. INTRODUCTION

Many of transition-metal oxides are good insulators, even though their d band is only partly filled. At low temperatures, they often exhibit some antiferromagnetic spin ordering but remain insulating well above the Néel temperatures where the spin ordering has completely disappeared.¹ An insulating antiferromagnetic state may be well described by

Slater's split-band model,² but the band gap involved is proportional to the sublattice magnetization and hence vanishes as the antiferromagnetic spin ordering disappears. Therefore, this model is incapable of describing the insulating state of transition-metal oxides properly.

Hubbard^{3,4} suggested that such an insulating state is a consequence of strong correlation effects in d bands. He further argued that, since the intra-

atomic interaction I in the iron-group elements is of the order 5–10 eV and larger than the width of the d band, even many-body perturbation expansions may not be able to handle the interaction correctly. Thus he applied the Green's-function method developed by Zubarev⁵ and solved the equation of motion for the one-particle Green's function in such a way that solutions give the correct description of atoms involved in the limit of an infinitely large lattice parameter. The results obtained by Hubbard are, in fact, quite different from perturbation results and exhibit the splitting of bands in the absence of magnetization and under a finite lattice parameter. As the lattice parameter decreases and the density of electrons increases, the band gap of the improved version of his solutions decreases and vanishes, demonstrating a nonmetal-to-metal transition.⁴

As Herring⁶ has suggested, a Hubbard-like approach should be appropriate to describe the insulating state of transition-metal oxides since the d band has the sole responsibility for both electrical and magnetic properties of these materials. The lattice, however, exhibits insulating antiferromagnetism in its ground state, while the Hubbard solutions are limited to a nonmagnetic state. Since the Hubbard mechanism responsible for creating the insulating state is the dynamical interaction between two electrons which happen to meet at the same atomic site, the interaction can become stronger than the Hartree-Fock interaction responsible for Slater-type antiferromagnetism. Thus we can expect the insulating characteristics to stay longer than the magnetic ordering at higher temperatures.

In this paper, we shall solve the Hubbard Hamiltonian in the presence of sublattice magnetization and show that an original nonmagnetic band splits into spin-polarized bands just as in Slater's model. In fact, the split bands become asymptotically equal to Slater's split-band solutions in the limit of the fully antiferromagnetic state. As the sublattice magnetization decreases, the band gap of Slater's model will decrease, while in the present model the gap, being generated by the Hubbard interaction, remains constant and instead antipolarized bands will appear and increase their strength. In the limit of vanishingly small magnetization, the strengths of the antipolarized bands will become equal to those of the polarized bands, yielding Hubbard's nonmagnetic insulating state.

II. ANTIFERROMAGNETIC SOLUTION UNDER THE HUBBARD APPROXIMATION

The Hamiltonian used in the Hubbard model³ is

$$\mathcal{H} = \sum_{RR'\sigma} \epsilon_{RR'} c_{R\sigma}^\dagger c_{R'\sigma} + I \sum_R \mathfrak{N}_R \mathfrak{N}_{R_1}, \quad (2.1)$$

where R, R' label the lattice points, $c_{R\sigma}^\dagger, c_{R\sigma}$ are creation and annihilation operators for an electron

of spin $\sigma = \uparrow$ or \downarrow in the Wannier state on atom R , and $\mathfrak{N}_{R\sigma} = c_{R\sigma}^\dagger c_{R\sigma}$ is the number of electrons in the state $R\sigma$. The first term in \mathcal{H} describes hopping or kinetic energy and is diagonalized by a set of Bloch functions. This is possible because the translation periodicity of the lattice makes $\epsilon_{RR'}$ a function of the distance $R - R'$ only. The second term gives a repulsive interaction between two electrons on the same site, and I is the measure of the interaction and a positive constant.

We shall use the energy Fourier transform of the one-particle double-time Green's function⁵:

$$G_{RR}^\sigma \equiv \langle\langle c_{R\sigma}; c_{R'\sigma}^\dagger \rangle\rangle_E, \quad (2.2)$$

for the calculation of excitation spectra of the system. To calculate this Green's function, however, it is more convenient to construct the equations of motion for the Green's functions:

$$\Gamma_{RR'}^{(\pm)\sigma} \equiv \langle\langle c_{R\sigma} \mathfrak{N}_{R\bar{\sigma}}^{(\pm)}; c_{R'\sigma}^\dagger \rangle\rangle_E, \quad (2.3)$$

where the spin $\bar{\sigma}$ is opposite to σ and

$$\mathfrak{N}_{R\sigma}^{(+)} \equiv \mathfrak{N}_{R\sigma}, \quad \mathfrak{N}_{R\sigma}^{(-)} \equiv 1 - \mathfrak{N}_{R\sigma}. \quad (2.4)$$

The desired Green's function $G_{RR'}^\sigma$ can then be generated from the above two functions by the trivial relation

$$G_{RR'}^\sigma = \Gamma_{RR'}^{(+)\sigma} + \Gamma_{RR'}^{(-)\sigma}. \quad (2.5)$$

With the Hamiltonian (2.1), the equations of motion for $\Gamma_{RR'}^{(\pm)\sigma}$ come out to be

$$\begin{aligned} E \langle\langle c_{R\sigma} \mathfrak{N}_{R\bar{\sigma}}^{(\pm)}; c_{R'\sigma}^\dagger \rangle\rangle_E &= (\delta_{RR'} / 2\pi) \langle \mathfrak{N}_{R\bar{\sigma}}^{(\pm)} \rangle \\ &+ \sum_{R''} \epsilon_{RR''} \langle\langle c_{R''\sigma} \mathfrak{N}_{R\bar{\sigma}}^{(\pm)}; c_{R'\sigma}^\dagger \rangle\rangle_E \\ &+ \delta^{(\pm)} I \langle\langle c_{R\sigma} \mathfrak{N}_{R\bar{\sigma}}; c_{R'\sigma}^\dagger \rangle\rangle_E \\ &+ \sum_{R''} (\epsilon_{RR''} \langle\langle c_{R\sigma} c_{R\bar{\sigma}}^\dagger c_{R''\bar{\sigma}}; c_{R'\sigma}^\dagger \rangle\rangle_E \\ &- \epsilon_{R''R} \langle\langle c_{R\sigma} c_{R''\bar{\sigma}}^\dagger c_{R\bar{\sigma}}; c_{R'\sigma}^\dagger \rangle\rangle_E), \quad (2.6) \end{aligned}$$

where $\delta^{(+)} = 1$ for the equation of $\Gamma_{RR'}^{(+)\sigma}$, but $\delta^{(+)} = 0$ for that of $\Gamma_{RR'}^{(-)\sigma}$, illustrating the absence of the term involving I in the equation of $\Gamma_{RR'}^{(-)\sigma}$.

The above equations are those used by Hubbard, and his results may be reproduced if one assumes that the mean number of electrons at a lattice site, $\langle \mathfrak{N}_{R\sigma} \rangle$, is a constant independent of the site and the spin, that is,

$$\langle \mathfrak{N}_{R_1} \rangle = \langle \mathfrak{N}_{R_2} \rangle = \frac{1}{2} n. \quad (2.7)$$

Consequently, his results are applicable to a nonmagnetic state only.

Here we assume a two-sublattice structure such that the nearest neighbors of an atom on sublattice A are on sublattice B and vice versa. Let $R(A)$ and $R(B)$ be atoms in sublattices A and B , respectively, and assume a finite sublattice magnetization M . Hence the density of electrons with up- and down-spins at a lattice point $R(A)$ in sublattice A , de-

noted by $\langle \mathfrak{N}_{R(A)\uparrow} \rangle$ and $\langle \mathfrak{N}_{R(A)\downarrow} \rangle$, respectively, are constant and equal to the density of electrons with down- and up-spins at a lattice point $R(B)$ in sublattice B , $\langle \mathfrak{N}_{R(B)\uparrow} \rangle$ and $\langle \mathfrak{N}_{R(B)\downarrow} \rangle$. That is,

$$\langle \mathfrak{N}_{R(A)\uparrow} \rangle = \langle \mathfrak{N}_{R(B)\uparrow} \rangle = \left(\frac{1}{2} + \varepsilon\right)n, \quad (2.8)$$

$$\langle \mathfrak{N}_{R(A)\downarrow} \rangle = \langle \mathfrak{N}_{R(B)\downarrow} \rangle = \left(\frac{1}{2} - \varepsilon\right)n, \quad (2.9)$$

where the total density of electrons at a lattice point, n , is a constant independent of the sublattice magnetization M , while $2\varepsilon n$ gives the value of M per atom:

$$n = \langle \mathfrak{N}_{R(A)\uparrow} \rangle + \langle \mathfrak{N}_{R(A)\downarrow} \rangle = \langle \mathfrak{N}_{R(B)\uparrow} \rangle + \langle \mathfrak{N}_{R(B)\downarrow} \rangle, \quad (2.10)$$

$$M = 2\varepsilon n = \langle \mathfrak{N}_{R(A)\uparrow} \rangle - \langle \mathfrak{N}_{R(A)\downarrow} \rangle = \langle \mathfrak{N}_{R(B)\uparrow} \rangle - \langle \mathfrak{N}_{R(B)\downarrow} \rangle. \quad (2.11)$$

We shall solve Eqs. (2.6) under the assumption (2.8) and (2.9). In addition, we shall introduce the decoupling approximations used by Hubbard in his first paper. These are to assume that (i) if $R'' \neq R$, the Green's function $\langle\langle c_{R''\sigma} \mathfrak{N}_{R\bar{\sigma}}^{(\pm)}; c_{R'\sigma}^\dagger \rangle\rangle_E$ which appears on the right-hand side of Eq. (2.6) can be decomposed into a product such that

$$\begin{aligned} \langle\langle c_{R''\sigma} \mathfrak{N}_{R\bar{\sigma}}^{(\pm)}; c_{R'\sigma}^\dagger \rangle\rangle_E &= \langle \mathfrak{N}_{R\bar{\sigma}}^{(\pm)} \rangle G_{R''R'}^\sigma \quad \text{when } R'' \neq R \\ &= \Gamma_{RR'}^{(\pm)\sigma} \quad \text{when } R'' = R, \end{aligned} \quad (2.12)$$

and (ii) the last two Green's functions on the right-hand side of Eq. (2.6), which involve four c 's, can be neglected:

$$\langle\langle c_{R\sigma} c_{R\bar{\sigma}}^\dagger c_{R'\bar{\sigma}}; c_{R'\sigma}^\dagger \rangle\rangle_E = \langle\langle c_{R\sigma} c_{R'\bar{\sigma}}^\dagger c_{R\bar{\sigma}}; c_{R'\sigma}^\dagger \rangle\rangle_E = 0, \quad (2.13)$$

where $R'' \neq R$. As has been pointed out by Hubbard,⁴ the above decoupling scheme has the disadvantage that solutions obtained may remain insulating and the metal-nonmetal transition may not be demonstrated. Since we are not interested in the Mott transition but rather in the transition from an antiferromagnetic insulator to a nonmagnetic insulator, the above approximations may be sufficient for our purpose of demonstrating essential differences between Slater's two-band model of antiferromagnetism and the Hubbard-type insulating solution. Even more sophisticated decoupling schemes do not have mathematical justification, and, if the Hubbard solutions have any validity at all, the following results would reflect the characteristics of the Hubbard solutions.⁷

The approximations described above reduce the original equations (2.6) to the following form:

$$\begin{aligned} (E - T_0 - \delta^{(*)}) \Gamma_{RR'}^{(\pm)\sigma} &= (\delta_{RR'}/2\pi) \langle \mathfrak{N}_{R\bar{\sigma}}^{(\pm)} \rangle \\ &+ \langle \mathfrak{N}_{R\bar{\sigma}}^{(\pm)} \rangle \sum_{R''} t_{RR''} G_{R''R'}^\sigma, \end{aligned} \quad (2.14)$$

where the new notation

$$T_0 \equiv \epsilon_{RR}, \quad t_{RR'} \equiv \epsilon_{RR'} - \epsilon_{RR} \delta_{RR'} \quad (2.15)$$

is introduced to facilitate the Fourier transformation of the original equations under the approximation (2.12). Here the spin $\bar{\sigma}$ involved in $\mathfrak{N}_{R\bar{\sigma}}^{(\pm)}$ is opposite of the spin σ involved in the Green's function $G_{RR'}^\sigma$ and the average value $\langle \mathfrak{N}_{R\bar{\sigma}}^{(\pm)} \rangle$ is given by Eqs. (2.8) and (2.9).

The sublattice magnetization reduces the symmetry of the lattice by forcing two neighboring unit cells of the nonmagnetic state to form a single magnetic unit cell. This, in turn, introduces a single translational vector Q in the reciprocal lattice of the antiferromagnetic state and splits the nonmagnetic band into two subbands. Hence any Bloch function $\tilde{\psi}_k$ for the split bands can be represented in terms of the Bloch functions ψ_k of the original band by

$$\begin{aligned} \tilde{\psi}_k &= \psi_k \cos \theta_k + \psi_{k+Q} \cos \theta_k, \\ \tilde{\psi}_{k+Q} &= -\psi_k \sin \theta_k + \psi_{k+Q} \cos \theta_k, \end{aligned} \quad (2.16)$$

where $\theta_k \equiv \theta_{k\sigma}$ is an arbitrary spin-dependent parameter to be determined later, and k runs over the inner-half-zone and $k+Q$ is the corresponding wave vector of the outer half-zone. The Fourier transformation, which takes $c_{R\sigma}$, $c_{R\sigma} N_{R\bar{\sigma}}$ to

$$c_{k\sigma} = N^{-1/2} \sum_R e^{ikR} c_{R\sigma}, \quad (2.17)$$

$$(c\mathfrak{N})_{k\sigma} = N^{-1/2} \sum_R e^{ikR} c_{R\sigma} \mathfrak{N}_{R\bar{\sigma}}, \quad (2.18)$$

will then transform Eq. (2.14) into the following form:

$$(E - T_0 - \delta^{(*)}) \underline{\Gamma}^{(\pm)\sigma} = (1/2\pi) \underline{n}^{(\pm)\sigma} + \underline{n}^{(\pm)\sigma} \underline{t} \underline{G}^\sigma. \quad (2.19)$$

Here we have used the matrix representation merely to represent eight equations for eight distinct $\Gamma_{kk}^{(\pm)\sigma}$, $\Gamma_{kk+Q}^{(\pm)\sigma}$, ... by regarding them as the (1, 1), (1, 2), ... elements of the 2×2 matrices $\underline{\Gamma}^{(\pm)\sigma}$. The notation used is as follows:

$$\begin{aligned} \underline{\Gamma}^{(\pm)\sigma} &= \begin{pmatrix} \Gamma_{kk}^{(\pm)\sigma} & \Gamma_{kk+Q}^{(\pm)\sigma} \\ \Gamma_{k+Qk}^{(\pm)\sigma} & \Gamma_{k+Qk+Q}^{(\pm)\sigma} \end{pmatrix}, \quad \underline{G}^\sigma = \begin{pmatrix} G_{kk}^\sigma & G_{kk+Q}^\sigma \\ G_{k+Qk}^\sigma & G_{k+Qk+Q}^\sigma \end{pmatrix}, \\ \underline{n}^{(+)\sigma} &= \begin{pmatrix} \frac{1}{2}n & \pm \varepsilon n \\ \pm \varepsilon n & \frac{1}{2}n \end{pmatrix}, \end{aligned} \quad (2.20)$$

$$\underline{n}^{(-)\sigma} = \underline{1} - \underline{n}^{(+)\sigma} = \begin{pmatrix} 1 - \frac{1}{2}n & \mp \varepsilon n \\ \mp \varepsilon n & 1 - \frac{1}{2}n \end{pmatrix}, \quad \underline{t} = \begin{pmatrix} t_k & 0 \\ 0 & t_{k+Q} \end{pmatrix},$$

where upper signs involved in the expressions for $\underline{n}^{(+)\sigma}$ and $\underline{n}^{(-)\sigma}$ are taken for $\sigma = \uparrow$ and lower signs for $\sigma = \downarrow$ and

$$t_k = \sum_R e^{ik(R-R')} t_{RR'},$$

while $\Gamma_{kk}^{(\pm)\sigma}$, G_{kk}^σ , etc., are obtained from $\Gamma_{RR'}^{(\pm)\sigma}$ and $G_{RR'}^\sigma$, respectively, by replacing $c_{R\sigma}$, $c_{R\sigma} \mathfrak{N}_{R\bar{\sigma}}$, etc.,

by $c_{k\sigma}$, $(c\mathcal{N})_{k\sigma}$, etc. The simple relation (2.5) is still valid for $\underline{\Gamma}^{(+)\sigma}$ and hence

$$\underline{G}^\sigma = \underline{\Gamma}^{(+)\sigma} + \underline{\Gamma}^{(-)\sigma}. \quad (2.21)$$

By inserting (2.19) into (2.21), we find the one-particle Green's functions \underline{G}^σ to be given by

$$(\underline{F}^\sigma - \underline{t}) \underline{G}^\sigma = \underline{1}/2\pi, \quad (2.22)$$

where

$$(\underline{F}^\sigma)^{-1} = \frac{\underline{n}^{(+)\bar{\sigma}}}{E - T_0 - I} + \frac{\underline{n}^{(-)\bar{\sigma}}}{E - T_0}. \quad (2.23)$$

The form of the above equation is the same as that obtained for a nonmagnetic state by Hubbard under the simplest decoupling scheme, but the present equation is spin-dependent and written in the

$$\begin{aligned} (\underline{\tilde{F}}^\sigma - \underline{\tilde{t}}) &= \underline{U}^\dagger (\underline{F}^\sigma - \underline{t}) \underline{U} \\ &= \begin{pmatrix} L + \Delta L^\sigma \sin 2\theta_k - t_k \cos^2 \theta_k - t_{k+Q} \sin^2 \theta_k, & \Delta L^\sigma \cos 2\theta_k - \frac{1}{2}(t_{k+\theta} - t_k) \sin 2\theta_k \\ \Delta L^\sigma \cos 2\theta_k - \frac{1}{2}(t_{k+Q} - t_k) \sin 2\theta_k, & L - \Delta L^\sigma \sin 2\theta_k - t_k \sin^2 \theta_k - t_{k+Q} \cos^2 \theta_k \end{pmatrix}, \end{aligned} \quad (2.25)$$

where

$$L \equiv \frac{(E - T_0)(E - T_0 - I)[E - T_0 - (1 - \frac{1}{2}n)I]}{[E - T_0 - (1 - \frac{1}{2}n + n\varepsilon)I][E - T_0 - (1 - \frac{1}{2}n - n\varepsilon)I]}, \quad (2.26)$$

ΔL^σ

$$\equiv \pm \frac{(E - T_0)(E - T_0 - I)n\varepsilon I}{[E - T_0 - (1 - \frac{1}{2}n + n\varepsilon)I][E - T_0 - (1 - \frac{1}{2}n - n\varepsilon)I]}, \quad (2.27)$$

and the (+) sign is for $\Delta L'$ and the (-) sign for $\Delta L''$. In order to make the matrix $(\underline{F}^\sigma - \underline{t})$ diagonal, the parameter θ_k involved in \underline{U} should be determined by

$$\tan 2\theta_{k\sigma} = 2\Delta L^\sigma / (t_{k+Q} - t_k), \quad (2.28)$$

and consequently, $\theta_{k_1} = -\theta_{k_2}$. The Green's functions are then written as

$$(L + \Delta L^\sigma \sin 2\theta_k - t_k \cos^2 \theta_k - t_{k+Q} \sin^2 \theta_k) G_{kk}^\sigma = 1/2\pi, \quad (2.29)$$

$$(L - \Delta L^\sigma \sin 2\theta_k - t_k \sin^2 \theta_k - t_{k+Q} \cos^2 \theta_k) G_{k+Q, k+Q}^\sigma = 1/2\pi, \quad (2.30)$$

where G_{kk}^σ gives the spectra of the inner half-zone and $G_{k+Q, k+Q}^\sigma$ those of the outer half-zone. The above two equations are now effectively spin independent as $\Delta L' \sin 2\theta_{k_1} = \Delta L'' \sin 2\theta_{k_2}$. Before we start to investigate the nature of the spectra obtained above in Sec. IV, we shall demonstrate how Slater's split-band model² will come out by the present method. This will make it easy to compare the present results with the Hartree-Fock solutions by Slater and illuminate the characteristics of the Hubbard-type

matrix representation, and hence the equation for G_{kk}^σ , for instance, involves $G_{k+Q, k}^\sigma$ and so on. This is a consequence of the sublattice magnetization, which has split the reciprocal lattice of the nonmagnetic state in two, creating the coupling between the two states k and $k+Q$. The expression for the Green's function G_{kk}^σ will be obtained by diagonalizing the matrix $(\underline{F}^\sigma - \underline{t})$ by a unitary transformation:

$$\underline{U} = \begin{pmatrix} \cos \theta_k & -\sin \theta_k \\ \sin \theta_k & \cos \theta_k \end{pmatrix}, \quad (2.24)$$

which takes c_k to $\tilde{c}_k = c_k \cos \theta_k + c_{k+Q} \sin \theta_k$ and the original Bloch function ψ_k to $\tilde{\psi}_k$ of the split bands. After a straightforward calculation, we find that the matrix $(\underline{\tilde{F}}^\sigma - \underline{\tilde{t}})$ in the split-band scheme should have the following form:

solutions in the presence of an antiferromagnetic ordering.

III. HARTREE-FOCK APPROXIMATION: SLATER'S SPLIT-BAND MODEL

The qualitative formulation of Slater's model, undertaken by Matsubara and Yokota,⁸ may be reproduced by the present method if the Hartree-Fock effective Hamiltonian is used in place of the original Hubbard Hamiltonian (2.1). The Hartree-Fock effective Hamiltonian may be generated from Eq. (2.1) by replacing the interaction term $\mathfrak{N}_{R\sigma} \mathfrak{N}_{R\bar{\sigma}}$ by $\mathfrak{N}_{R\sigma} \langle \mathfrak{N}_{R\bar{\sigma}} \rangle + \mathfrak{N}_{R\bar{\sigma}} \langle \mathfrak{N}_{R\sigma} \rangle$:

$$\mathfrak{H}_{\text{HF}} = \sum_{RR'\sigma} \epsilon_{RR'} c_{R\sigma}^\dagger c_{R'\sigma} + I \sum_{R\sigma} \mathfrak{N}_{R\sigma} \langle \mathfrak{N}_{R\bar{\sigma}} \rangle. \quad (3.1)$$

The equation of motion for the Green's function $G_{RR'}^\sigma$ turns out to be

$$(E - T_0 - \langle \mathfrak{N}_{R\bar{\sigma}} \rangle I) G_{RR'}^\sigma = \delta_{RR'} / 2\pi + \sum_{R''} t_{RR''} G_{R''R'}^\sigma, \quad (3.2)$$

and it can be solved exactly. In the presence of the sublattice magnetization described by Eqs. (2.8) and (2.9), the Fourier transform of Eq. (3.2) can be written in the form

$$(\underline{F}_{\text{HF}}^\sigma - \underline{t}) \underline{G}^\sigma = \underline{1}/2\pi, \quad (3.3)$$

which is similar to the result (2.22) in Sec. II except that the matrix \underline{F}^σ has been replaced by $\underline{F}_{\text{HF}}^\sigma$:

$$\underline{F}_{\text{HF}}^\sigma = \underline{1}(E - T_0) - \underline{n}^{(+)\bar{\sigma}} I. \quad (3.4)$$

Again, the Green's functions G_{kk}^σ and $G_{k+Q, k+Q}^\sigma$ may be obtained by a unitary transformation which makes the matrix $(\underline{F}_{\text{HF}}^\sigma - \underline{t})$ diagonal. The parameter $\theta_{k\sigma}$ of the unitary matrix \underline{U} is then given by

$$\tan 2\theta_{k\sigma} = \frac{2\Delta L_{(0)}^\sigma}{t_{k+Q} - t_k}, \quad \Delta L_{(0)}^\sigma = \pm n\varepsilon I, \quad (3.5)$$

instead of Eq. (2.28), and we find that

$$(E - T_0 - \frac{1}{2}nI + \Delta L_{(0)}^\sigma \sin 2\theta_k - t_k \cos^2 \theta_k - t_{k+Q} \sin^2 \theta_k) G_{kk}^\sigma = 1/2\pi, \quad (3.6)$$

$$(E - T_0 - \frac{1}{2}nI - \Delta L_{(0)}^\sigma \sin 2\theta_k - t_k \sin^2 \theta_k - t_{k+Q} \cos^2 \theta_k) G_{k+Q, k+Q}^\sigma = 1/2\pi. \quad (3.7)$$

Let us assume, for simplicity, a finite energy gap between the split bands so that all states k in the inner half-zone lie below any of the states in the outer half-zone. When the number of electrons nN is less than the number of atoms N , the lower band will be filled up to the Fermi state k_F , leaving the upper band empty. The magnetization M can be calculated from the difference in the densities of electrons with up- and down-spins:

$$M = 2\varepsilon n = 2N^{-1} \sum_k^{k_F} \sin 2\theta_k, \quad (3.8)$$

and the total energy \mathcal{E} is given by

$$\mathcal{E} = \text{const} + 2 \sum_k^{k_F} (t_k \cos^2 \theta_k + t_{k+Q} \sin^2 \theta_k) - \frac{I}{N} \left(\sum_k^{k_F} \sin 2\theta_k \right)^2. \quad (3.9)$$

By using the expression (3.5) for θ_k in Eqs. (3.6) and (3.7), the Hartree-Fock energy parameters in the antiferromagnetic state are written as

$$E_k - T_0 = \frac{1}{2}nI + \frac{1}{2}(t_k + t_{k+Q}) \pm \frac{1}{2} [M^2 I^2 + (t_{k+Q} - t_k)^2]^{1/2}, \quad (3.10)$$

where the magnetization M should be determined self-consistently by Eq. (3.8), that is,

$$\frac{2I_0}{N} \sum_k^{k_F} [M^2 I^2 + (t_{k+Q} - t_k)^2]^{-1/2} = 1. \quad (3.11)$$

If the number of electrons nN exceeds N , we have to make only trivial modifications to Eqs. (3.8), (3.9), and (3.11), so that the summations extend over the upper band. The results obtained here are parallel to those obtained by Matsubara and Yokota and by des Cloizeaux.⁹ Since the present results are exact solutions of the Hartree-Fock effective Hamiltonian, the optimum condition for parameter θ_k , Eq. (3.5), is valid independent of the Fermi energy and the number of electrons involved. In fact, the results obtained here are valid even if the two split bands overlap, provided the summation extends over the two bands simultaneously up to the Fermi level. The procedure of calculating the condition (3.5) followed by des Cloizeaux as well as Matsubara and Yokota is to minimize the expression for the total energy \mathcal{E} and hence their results appear

to be meaningful only when the inner shell is completely filled and the lattice exhibits insulating anti-ferromagnetism.

The Hartree-Fock approximation in the present formulation is to replace the Hubbard-type operator \underline{F}^σ , which describes the resonant properties of atoms, by the Hartree-Fock average $\underline{F}_{\text{HF}}^\sigma$. In the limit of $n = 1$ or 0 , the resonant operator \underline{F}^σ becomes identical to the Hartree-Fock average $\underline{F}_{\text{HF}}^\sigma$. If the intra-atomic interaction I is small as compared with bandwidth parameter t_k , the resonant operator \underline{F}^σ will also approach the Hartree-Fock average $\underline{F}_{\text{HF}}^\sigma$ asymptotically. In these limits, therefore, Hubbard-type solutions should reproduce the Hartree-Fock results obtained here.

IV. ASYMPTOTIC EXPANSIONS OF ANTIFERROMAGNETIC SOLUTION

Let us now investigate the asymptotic behavior of the Hubbard-type solutions in the presence of sublattice magnetization, and expand them in a power series. The Green's functions G_{kk}^σ and $G_{k+Q, k+Q}^\sigma$, given by Eqs. (2.29) and (2.30), may be written in the form

$$G_{\tau\tau} = \frac{1}{2\pi} \left(\frac{A_1(\tau)}{\xi - \xi_1(\tau)} + \frac{A_2(\tau)}{\xi - \xi_2(\tau)} + \frac{A_3(\tau)}{\xi - \xi_3(\tau)} \right), \quad (4.1)$$

for $\tau = k$ and $k + Q$, where $\xi \equiv E - T_0$. The coefficients $A_1(\tau)$, $A_2(\tau)$, $A_3(\tau)$ yield the probabilities of finding the states described by $\xi_1(\tau)$, $\xi_2(\tau)$, $\xi_3(\tau)$, respectively, and hence are positive and obey the condition

$$A_1(\tau) + A_2(\tau) + A_3(\tau) = 1. \quad (4.2)$$

Use of the explicit expressions (2.26) and (2.27) leads to

$$A_a(\tau) = \frac{[\xi_a(\tau) - (1 - \frac{1}{2}n + n\varepsilon)I][\xi_a(\tau) - (1 - \frac{1}{2}n - n\varepsilon)I]}{[\xi_a(\tau) - \xi_b(\tau)][\xi_a(\tau) - \xi_c(\tau)]}, \quad (4.3)$$

where a, b, c , respectively, take 1, 2, 3, or 2, 3, 1, or 3, 1, 2, while the three roots $\xi_1(\tau) < \xi_2(\tau) < \xi_3(\tau)$ are obtained by solving the cubic equations

$$f_\tau[\xi] \equiv \xi(\xi - I)[\xi - (1 - \frac{1}{2}n \mp n\varepsilon \sin 2\theta_k)I] - \eta_\tau[\xi - (1 - \frac{1}{2}n + n\varepsilon)I][\xi - (1 - \frac{1}{2}n - n\varepsilon)I] = 0. \quad (4.4)$$

Here the upper sign ($-$) is for $\tau = k$, the lower sign ($+$) for $\tau = k + Q$, and

$$\eta_k \equiv t_k \cos^2 \theta_k + t_{k+Q} \sin^2 \theta_k, \quad \eta_{k+Q} \equiv t_k \sin^2 \theta_k + t_{k+Q} \cos^2 \theta_k. \quad (4.5)$$

Figures 1 and 2 show the schematic behavior of $f_\tau[\xi]$ as a function of ξ . Especially, we note that $f_\tau[\xi = \infty] = \infty$, $f_\tau[\xi = -\infty] = -\infty$, $f_\tau[\xi = (1 - \frac{1}{2}n - n\varepsilon)I] > 0$, and $f_\tau[\xi = (1 - \frac{1}{2}n + n\varepsilon)I] < 0$, while the signs of $f_\tau[\xi]$, for $\xi = 0, (1 - \frac{1}{2}n \mp n\varepsilon \sin 2\theta_k)I$,

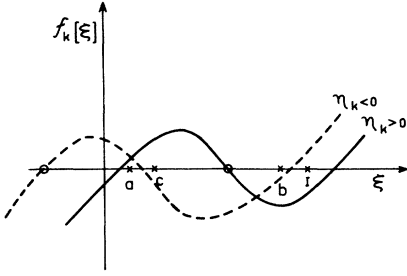


FIG. 1. $f_k[\xi]$ as a function of ξ , where $n \approx \frac{1}{2}$, $\varepsilon \approx \frac{1}{8}$, $a = (1 - \frac{1}{2}n - n\varepsilon)I$, $b = (1 - \frac{1}{2}n + n\varepsilon)I$, $c = (1 - \frac{1}{2}n - n\varepsilon \sin 2\theta_k)I$. The k -dependent solutions of $f_k[\xi] = 0$ are marked by \circ .

and I , are determined by the sign of η_τ as illustrated in the figures. Since $0 < \varepsilon < \frac{1}{2}$ and $0 < n < 2$, the order of the three points

$$(1 - \frac{1}{2}n - n\varepsilon)I, \quad (1 - \frac{1}{2}n \mp n\varepsilon \sin 2\theta_k)I, \quad (1 - \frac{1}{2}n + n\varepsilon)I,$$

is fixed on the abscissa and lies between 0 and I , yielding the following bounds for each of the solutions $\xi_a(\tau)$.

For $\eta_\tau > 0$, we have

$$\begin{aligned} 0 < \xi_1(\tau) < (1 - \frac{1}{2}n - n\varepsilon)I, \\ (1 - \frac{1}{2}n \mp n\varepsilon \sin 2\theta_k)I < \xi_2(\tau) < (1 - \frac{1}{2}n + n\varepsilon)I, \quad (4.6) \\ I < \xi_3(\tau). \end{aligned}$$

For $\eta_\tau < 0$, we have

$$\begin{aligned} \xi_1(\tau) < 0, \\ (1 - \frac{1}{2}n - n\varepsilon)I < \xi_2(\tau) < (1 - \frac{1}{2}n \mp n\varepsilon \sin 2\theta_k)I, \quad (4.7) \\ (1 - \frac{1}{2}n + n\varepsilon)I < \xi_3(\tau) < I. \end{aligned}$$

The above inequalities imply immediately that (i) if the band is nearly empty (small n) and $\eta_\tau < 0$, both $\xi_2(\tau)$ and $\xi_3(\tau)$ approach I and $\xi_1(\tau)$ approaches the Hartree-Fock result t_τ regardless of the value of ε since θ_k of $\xi_1(\tau)$ determined by Eq. (2.28) vanishes. As we shall see in Eq. (4.11a) following, this is also true for $\eta_\tau > 0$. (ii) If the band is nearly full ($n \approx 2$) and $\eta_\tau > 0$, ε becomes zero and $\xi_1(\tau)$ and $\xi_2(\tau)$ approach zero, while $\xi_3(\tau)$ approaches the Hartree-Fock value t_τ . This will be also true for $\eta_\tau < 0$, as is seen in Eq. (4.17b). (iii) If ε is small, the bounds for $\xi_2(\tau)$ will become stringent, making $\xi_2(\tau)$ nearly a constant independent of k , that is, $\approx (1 - \frac{1}{2}n)I$, regardless of the density n of electrons in the band. However, the probability of finding such a state, $A_2(\tau)$, is vanishingly small.

Since the three roots are bounded separately, Eq. (4.4) may be solved by successive approximation. For instance, the lower two solutions $\xi_1(k)$ and $\xi_2(k)$, for $\tau = k$, may be found by assuming that

$$c_3(\xi) = [\xi - (1 - \frac{1}{2}n + n\varepsilon)I] / (\xi - I) > 0 \quad (4.8)$$

is a slowly varying function when $\xi \approx \xi_1(\tau)$ or $\xi_2(\tau)$,

so that

$$\begin{aligned} \xi_1(k) \text{ or } \xi_2(k) = \frac{1}{2} \left[(1 - \frac{1}{2}n - n\varepsilon \sin 2\theta_k)I + c_3(\xi) \eta_k \right. \\ \left. \pm \left| (1 - \frac{1}{2}n - n\varepsilon \sin 2\theta_k)I - c_3(\xi) \eta_k \right| \right. \\ \left. \times \left(1 + \frac{4n\varepsilon(1 - \sin 2\theta_k)I c_3(\xi) \eta_k}{[(1 - \frac{1}{2}n - n\varepsilon \sin 2\theta_k)I - c_3(\xi) \eta_k]^2} \right)^{1/2} \right]. \quad (4.9) \end{aligned}$$

$\xi_1(k)$ and $\xi_2(k)$ may be calculated from Eqs. (4.8) and (4.9) self-consistently. If $\eta_k < 0$, the second term in $(\dots)^{1/2}$ on the right-hand side of (4.9) will be small for both the weakly magnetic case ($\varepsilon \rightarrow 0$) and the nearly fully magnetic case ($\varepsilon \approx \frac{1}{2} \sin 2\theta_k \approx \frac{1}{2}$), and $(\dots)^{1/2}$ may be expanded in a power series. The value of $c_3(\xi)$ will then be calculated easily, yielding the following results:

case(A) $\eta_k < 0$:

$$\xi_1(k) = (1 - \frac{1}{2}n + n\varepsilon) \eta_k - \dots, \quad (4.10a)$$

$$\xi_2(k) = (1 - \frac{1}{2}n - n\varepsilon \sin 2\theta_k)I + \dots. \quad (4.10b)$$

When $\eta_k > 0$, such an expansion is valid only if

$$(1 - \frac{1}{2}n - n\varepsilon \sin 2\theta_k)I \gg c_3(\xi) \eta_k, \quad \text{case (B1)}$$

or

$$(1 - \frac{1}{2}n - n\varepsilon \sin 2\theta_k)I \ll c_3(\xi) \eta_k, \quad \text{case (B2)}.$$

Solutions for case (B1) are the same as those for $\eta_k < 0$:

$$\text{case (B1) } \eta_k > 0; \quad (1 - \frac{1}{2}n - n\varepsilon \sin 2\theta_k)I > c_3(\xi) \eta_k:$$

$$\begin{aligned} \xi_1(k) = (1 - \frac{1}{2}n + n\varepsilon) \eta_k \\ \times \left(1 - \frac{n\varepsilon(1 - \sin 2\theta_k)I}{(1 - \frac{1}{2}n - n\varepsilon \sin 2\theta_k)I - (1 - \frac{1}{2}n + n\varepsilon) \eta_k} \right) \dots, \quad (4.11a) \end{aligned}$$

$$\begin{aligned} \xi_2(k) = (1 - \frac{1}{2}n - n\varepsilon \sin 2\theta_k)I \\ + \frac{n\varepsilon(1 - \sin 2\theta_k)I c_3(\xi_2) \eta_k}{(1 - \frac{1}{2}n - n\varepsilon \sin 2\theta_k)I - c_3(\xi_2) \eta_k} \dots, \quad (4.11b) \end{aligned}$$

with $c_3(\xi_2) \approx \varepsilon(1 + \sin 2\theta_k) / (\frac{1}{2} + \varepsilon \sin 2\theta_k)$. For case (B2), however, we have

$$\text{case (B2) } \eta_k > 0; \quad c_3(\xi) \eta_k > (1 - \frac{1}{2}n - n\varepsilon \sin 2\theta_k)I:$$

$$\xi_1(k) = (1 - \frac{1}{2}n - n\varepsilon)I$$

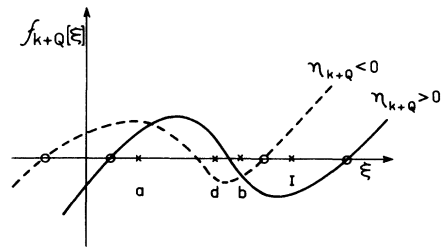


FIG. 2. $f_{k+Q}[\xi]$ as a function of ξ , where $n \approx \frac{1}{2}$, $\varepsilon \approx \frac{3}{8}$, $a = (1 - \frac{1}{2}n - n\varepsilon)I$, $b = (1 - \frac{1}{2}n + n\varepsilon)I$, $d = (1 - \frac{1}{2}n + n\varepsilon \sin 2\theta_k)I$. The k -dependent solutions of $f_{k+Q}[\xi] = 0$ are marked by \circ .

$$-\frac{n\varepsilon(1-\sin 2\theta_k)I(1-\frac{1}{2}n-n\varepsilon\sin 2\theta_k)I}{c_3(\xi_1)\eta_k-(1-\frac{1}{2}n-n\varepsilon\sin 2\theta_k)I}\dots, \quad (4.12a)$$

with

$$\xi_2(k) = (1 - \frac{1}{2}n + n\varepsilon)\eta_k \\ \times \left(1 + \frac{n\varepsilon(1-\sin 2\theta_k)I}{(1-\frac{1}{2}n+n\varepsilon)\eta_k - (1-\frac{1}{2}n-n\varepsilon\sin 2\theta_k)I} \right) \dots, \quad (4.12b)$$

$$c_3(\xi_1) \approx 2\varepsilon / (\frac{1}{2} + \varepsilon)I.$$

Here the second terms in the expansions are added since the denominator of the second term in $(\dots)^{1/2}$, being the difference between two quantities, is smaller than the case for $\eta_k < 0$. The corrections are useful in demonstrating the validity as well as limitations of the expansions used. In fact, it can be shown that the above results (and also the following results) satisfy the exact inequality relations (4.6) and (4.7). We note, in particular, that the leading term in (4.12a) was in the same form as that in (4.11b) but was modified by the correction term as it stands so that $\xi_1(k)$ is now shown to satisfy the required inequality (4.6). The third root $\xi_3(k)$ may be calculated similarly, yielding

$$\xi_3(k) = I + (\frac{1}{2}n - n\varepsilon)\eta_k I / (I + \eta_k) \dots \quad (4.13)$$

for both $\eta_k > 0$ and $\eta_k < 0$.

The above calculation may be extended for the cases with $\tau = k + Q$. We shall summarize the results in the following. The lowest root $\xi_1(k + Q)$ for both $\eta_{k+Q} > 0$ and $\eta_{k+Q} < 0$ is

$$\xi_1(k + Q) = (1 - \frac{1}{2}n - n\varepsilon)\eta_{k+Q} I / (I + \eta_{k+Q}) \dots \quad (4.14)$$

Then we have

case (C) $\eta_{k+Q} > 0$:

$$\xi_2(k + Q) = (1 - \frac{1}{2}n + n\varepsilon\sin 2\theta_k)I + \dots, \quad (4.15a)$$

$$\xi_3(k + Q) = I + (\frac{1}{2}n + n\varepsilon)\eta_{k+Q} - \dots; \quad (4.15b)$$

case (D1) $\eta_{k+Q} < 0$; $|c_1(\xi)\eta_{k+Q}| > (\frac{1}{2}n - n\varepsilon\sin 2\theta_k)I$:

$$\xi_2(k + Q) = (1 - n\varepsilon + n\varepsilon\sin 2\theta_k)I + (\frac{1}{2}n + n\varepsilon)\eta_{k+Q} \\ + \frac{n\varepsilon(1-\sin 2\theta_k)I(\frac{1}{2}n - n\varepsilon\sin 2\theta_k)I}{(\frac{1}{2}n + n\varepsilon)\eta_{k+Q} + (\frac{1}{2}n - n\varepsilon\sin 2\theta_k)I} \dots, \quad (4.16a)$$

$$\xi_3(k + \theta) = (1 - \frac{1}{2}n + n\varepsilon)I \\ - \frac{n\varepsilon(1-\sin 2\theta_k)I(\frac{1}{2}n - n\varepsilon\sin 2\theta_k)I}{c_1(\xi_3)\eta_{k+Q} + (\frac{1}{2}n - n\varepsilon\sin 2\theta_k)I} \dots; \quad (4.16b)$$

case (D2) $\eta_{k+Q} < 0$; $(\frac{1}{2}n - n\varepsilon\sin 2\theta_k)I > |c_1(\xi)\eta_{k+Q}|$:

$$\xi_2(k + Q) = (1 - \frac{1}{2}n + n\varepsilon\sin 2\theta_k)I \\ + \frac{n\varepsilon(1-\sin 2\theta_k)I c_1(\xi_2)\eta_{k+Q}}{(\frac{1}{2}n - n\varepsilon\sin 2\theta_k)I + c_1(\xi_2)\eta_{k+Q}} \dots, \quad (4.17a)$$

$$\xi_3(k + Q) = I + (\frac{1}{2}n + n\varepsilon)\eta_{k+Q}$$

$$-\frac{n\varepsilon(1-\sin 2\theta_k)I(\frac{1}{2}n + n\varepsilon)\eta_{k+Q}}{(\frac{1}{2}n - n\varepsilon\sin 2\theta_k)I + (\frac{1}{2}n + n\varepsilon)\eta_{k+Q}} \dots, \quad (4.17b)$$

where

$$c_1(\xi) = [\xi - (1 - \frac{1}{2}n - n\varepsilon)I] / \xi, \\ c_1(\xi_2) = n\varepsilon(1 + \sin 2\theta_k) / (1 - \frac{1}{2}n + n\varepsilon\sin 2\theta_k), \quad (4.18) \\ c_1(\xi_3) = 2n\varepsilon / (1 - \frac{1}{2}n + n\varepsilon).$$

The probabilities $A_a(\tau)$ of finding those states may be calculated easily by Eq. (4.3). The probability of finding the states whose energy spectra is given by $\xi(k) \approx (1 - \frac{1}{2}n + n\varepsilon)\eta_k$, that is, $\xi_1(k)$ in case of $\eta_k < (1 - \frac{1}{2}n - n\varepsilon\sin 2\theta_k)I$ and $\xi_2(k)$ in case of $\eta_k > (1 - \frac{1}{2}n - n\varepsilon\sin 2\theta_k)I$, is

$$A_{\text{low}}(k) \approx \frac{(1 - \frac{1}{2}n + n\varepsilon)(I - \eta_k)}{I - (1 - n + 2n\varepsilon)\eta_k}, \quad (4.19)$$

while, for $\xi_3(k)$,

$$A_{\text{up}}(k) = A_3(k) \approx \frac{(\frac{1}{2}n - n\varepsilon)(I + \eta_k)}{I - (1 - n + 2n\varepsilon)\eta_k}, \quad (4.20)$$

and, for nearly k -independent states,

$$A_c(k) \approx 0. \quad (4.21)$$

Similarly, for $\xi_1(k + Q)$, we find that

$$A_{\text{low}}(k + Q) = A_1(k + Q) \approx \frac{(1 - \frac{1}{2}n - n\varepsilon)(I - \eta_{k+Q})}{I - (1 - n - 2n\varepsilon)\eta_{k+Q}}, \quad (4.22)$$

and, for $\xi(k + Q) \approx I + (\frac{1}{2}n + n\varepsilon)\eta_{k+Q}$, that is, $\xi_2(k + Q)$ in case of $\eta_{k+Q} < -(\frac{1}{2}n - n\varepsilon\sin 2\theta_k)I$, and $\xi_3(k + Q)$ in case of $\eta_{k+Q} > -(\frac{1}{2}n - n\varepsilon\sin 2\theta_k)I$, we obtain

$$A_{\text{up}}(k + Q) \approx \frac{(\frac{1}{2}n + n\varepsilon)(I + \eta_{k+Q})}{I - (1 - n - 2n\varepsilon)\eta_{k+Q}}, \quad (4.23)$$

while, for nearly k -independent states,

$$A_c(k + Q) \approx 0. \quad (4.24)$$

V. NATURE OF THE SOLUTIONS AND DISCUSSIONS

To illustrate the nature of the solutions obtained in Sec. IV, we shall draw schematically the energy spectra assuming a simple band in which t_k increases monotonically as k increases from 0 to $2Q$. The Bloch energies in the sublattice structure, η_k and η_{k+Q} , are, as is seen from the definition (4.5), averages of t_k and t_{k+Q} . As magnetization M increases and θ_k defined by Eq. (2.8) increases, the deviations of η_k and η_{k+Q} from the unsplit-band energy t_k increase.

Under the perfect magnetization where $M = 1$ and $\theta_k = \frac{1}{2}\pi$, the present results reproduce the results of Slater's split-band model given in Sec. III; $\xi_1(k)$ for $\eta_k \leq (1 - n)I$ and $\xi_2(k)$ for $\eta_k \geq (1 - n)I$ give the Slater's lower band, and $\xi_2(k + Q)$ for $\eta_{k+Q} \leq 0$ and $\xi_3(k + Q)$ for $\eta_{k+Q} \geq 0$, the Slater's upper band, while the other solutions disappear altogether be-

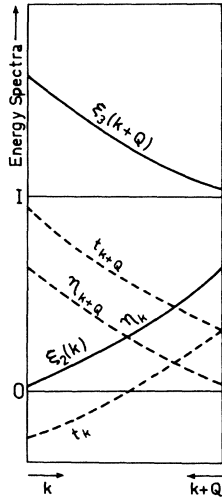


FIG. 3. Energy spectra $\xi_1(k)$, $\xi_3(k+Q)$, η_k , and η_{k+Q} for the fully magnetic case ($M=1$).

cause the probabilities of finding them, $A(\tau)$, vanish exactly. The two nonvanishing bands are separated by the intra-atomic interaction I as is shown in Fig. 3. If the number of electrons is the same as the number of atoms and $n=1$, the lower band is completely filled and the upper band is empty since $A_{1\text{ow}}(k) = A_{\text{up}}(k+Q) = 1$.

As the magnetization decreases from $M=1$ and ε decreases from the maximum value $\frac{1}{2}$, the values of the two boundaries $(1 - \frac{1}{2}n - n\varepsilon)I$ and $(1 - \frac{1}{2}n - n\varepsilon \sin 2\theta_k)I$ increase in parallel. The spectra $\xi_1(k)$ will behave like $(1 - \frac{1}{2}n + n\varepsilon)\eta_k$ when $c_3(\xi)\eta_k \ll (1 - \frac{1}{2}n - n\varepsilon \sin 2\theta_k)I$ but becomes $\sim (1 - \frac{1}{2}n - n\varepsilon)I$ when $c_3(\xi)\eta_k \gg (1 - \frac{1}{2}n - n\varepsilon \sin 2\theta_k)I$. The spectra $\xi_2(k)$, on the other hand, will stay constant $\sim (1 - \frac{1}{2}n - n\varepsilon \times \sin 2\theta_k)I$ when $c_3(\xi)\eta_k \ll (1 - \frac{1}{2}n - n\varepsilon \sin 2\theta_k)I$, but turn to $(1 - \frac{1}{2}n + n\varepsilon)\eta_k$ when $c_3(\xi)\eta_k \gg (1 - \frac{1}{2}n - n\varepsilon \times \sin 2\theta_k)I$. Our expansions are not valid in the intermediate region but the spectra may be interpolated as is shown in Fig. 4. The result looks as if the Slater's lower band is split into two by the Hubbard interaction.

According to the exact inequalities (4.6), there is a finite gap between $\xi_1(k)$ and $\xi_2(k)$ when $\theta_k \neq 0$, and hence the second term on the right-hand side of Eq. (4.9) will remain finite; in particular, the k -dependent part of this term will not vanish. Consequently, we can speculate that one of the two solutions of Eq. (4.9) maintains a k -dependent term much larger than $\frac{1}{2}(1 - \frac{1}{2}n + n\varepsilon)\eta_k$ and the other much smaller than $\frac{1}{2}(1 - \frac{1}{2}n + n\varepsilon)\eta_k$.

This implies a sharp splitting of the bands, and solutions of case B1 given by Eq. (4.11) will probably turn fairly quickly to those of case B2 given by Eq. (4.12) and vice versa at the "crossing point." Since the probability of finding k -dependent solutions, $A_C(k)$, is practically zero, this band splitting will introduce little physical consequences as long as the "crossing point" is far from the Fermi sur-

face. Thus the k -dependent parts of the two bands may be regarded as a quasi-single-band which corresponds to the Slater's lower band.

As magnetization M decreases, the "crossing point" moves upwards and eventually disappears leaving only the lower solution $\xi_1(k)$. At the same time, the k dependence of this Slater-like spin-polarized lower band decreases while the third spectra $\xi_1(k+Q)$, which was zero for all k in the fully magnetic state, will begin to acquire a k dependence. The probability density for the polarized lower band, $A_{1\text{ow}}(k)$, decreases from unity while that of the antipolarized lower band $\xi_1(k+Q)$, $A_{1\text{ow}}(k+Q)$, increases from zero and eventually these two become equal to the Hubbard value $A_{1\text{ow}}(\tau) \approx (I - \eta_\tau)/2I$, yielding Hubbard's nonmagnetic solution in the limit of $M=0$.

A similar splitting will appear in the Slater-like spin-polarized upper band because of the crossing of two types of solutions $\xi_2(k+Q)$ and $\xi_3(k+Q)$, provided $\eta_{k+Q} < 0$. The crossing point will appear near I when $M \approx 1$, and goes downwards as M decreases. At the same time, the polarized upper band becomes flatter and the third branch $\xi_3(k)$ appears. As the probability density $A_{\text{up}}(k+Q)$ decreases, $A_{\text{up}}(k)$ increases, and finally they become equal to the Hubbard value $A_{\text{up}}(\tau) \approx I + \eta_\tau/2I$ in the limit of $M=0$.

In the limit of $M=0$, η_k and η_{k+Q} become equal to t_k and t_{k+Q} , respectively, forming a continuously increasing single band t_k for $0 \leq k \leq 2Q$. The three boundaries $(1 - \frac{1}{2}n + n\varepsilon)I$, $(1 - \frac{1}{2}n \pm n\varepsilon \sin 2\theta_k)I$, and $(1 - \frac{1}{2}n - n\varepsilon)I$ are consolidated into a single boundary $(1 - \frac{1}{2}n)I$. The originally polarized and antipolarized lower bands, $\xi_1(k)$ and $\xi_1(k+Q)$, will lose the polarization and form a continuously increasing single lower band and lie below the boundary value $(1 - \frac{1}{2}n)I$, while the polarized and antipolarized

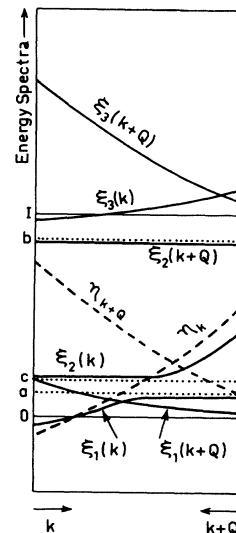


FIG. 4. Energy spectra for the intermediate case ($0 < M < 1$): $a = (1 - \frac{1}{2}n - n\varepsilon)I$, $b = (1 - \frac{1}{2}n + n\varepsilon)I$, and $c = (1 - \frac{1}{2}n - n\varepsilon \sin 2\theta_k)I$.

upper bands, $\xi_3(k)$ and $\xi_3(k+Q)$, will form a continuously increasing nonpolarized upper band and stay above the boundary $(1 - \frac{1}{2}n)I$. The other two solutions, $\xi_2(k)$ and $\xi_2(k+Q)$, having vanishing probability density $A_c(\tau) = 0$, disappear completely.

Since the probability density for the lower band, $A_{low}(\tau) \approx (I - \eta_\tau)/I$, is less than one, a system of N electrons and N atoms will not be an insulator because the lower band cannot accommodate all the N electrons. Herring⁶ speculates on this defect as if it were a fault of the Hubbard solution, but it might be a fault of the Hubbard model itself. The Hubbard Hamiltonian (2.1) has only the repulsive interaction I and no attractive force, so that it is not possible to create bound excitons responsible for the excitonic insulating state. With only the repulsive interaction, the lower band may not be able to accommodate all the N electrons as long as each of them carries a finite kinetic energy. This situation might be compared with the traffic on a highway. If the density of cars exceeds a certain limit, the flow of cars decreases suddenly, allowing stop and go motion only. To maintain an optimum flow, the density has to be below a critical value $(I - \eta_k)/I$, which should be much less than the maximum number of cars that can be piled on the highway.

In Slater's split-band model, the gap parameter MI is proportional to the magnetization, and as the magnetization decreases, the gap as well as the spin polarization decreases and, in the limit of $M = 0$, the gap disappears, yielding the nonmagnetic nonsplit band t_k . In the present results, the gap is introduced by the Hubbard interaction, which is a constant independent of the magnetization. As the magnetization M decreases, the k -dependent spin-polarized lower band, which is described by $\xi_1(k)$ or $\xi_2(k)$, and which has been responsible for stabilizing the fully magnetized state, is suppressed and the antipolarized band $\xi_1(k+Q)$, which is populated with electrons with opposite spins, will appear and its probability density, $A_{low}(k+Q)$, increases until the spin polarization of the system is completely cancelled and the Hubbard's nonmagnetic insulating state is obtained. This is precisely the reason why the system can remain insulating above the Néel point.

In the Hartree-Fock approximation, the kinetic and interaction energies can be identified separately, as in Eq. (3.9). In the present results, energy spectra contain both the kinetic and correlation energies and the total energy \mathcal{E} can be calculated by

$$\mathcal{E}/N = \int_0^n \xi_F(n) dn, \quad (5.1)$$

where $\xi_F(n)$ is the Fermi energy of the system containing nN electrons, that is,

$$\xi_F(n) = (1 - \frac{1}{2}n + n\epsilon)$$

$$\times (t_{k(n)} \cos^2 \theta_{k(n)} + t_{k(n)+Q} \sin^2 \theta_{k(n)}) \cdots, \quad (5.2)$$

when the lower-band contribution is being calculated. Here $\theta_{k(n)}$ is given by Eq. (2.28) and is a function of M , while $k(n)$ is defined on the basis of the original band t_k and is equal to the Fermi momentum of the system with nN electrons. The terms proportional to $(\frac{1}{2}n - n\epsilon)$ on the right-hand side of Eq. (5.2) give rise to the correlation energy. If the original nonsplit band t_k is given, then the total energy can be calculated by Eqs. (5.1) and (5.2) as a function of M . The magnetization M at the absolute zero of temperature will then be determined so as to make the total energy minimum.

As the temperature increases, the magnetization will decrease but very slowly until the temperature reaches a certain range near the Néel point. Then the magnetization will drop sharply. Before the sharp decrease of magnetization, the system may be represented by the highly spin-polarized lower band together with a small contribution from a weakly k -dependent antipolarized lower band as is shown in Fig. 4. As the temperature reaches the Néel point, the strength $A_{low}(k+Q)$ of the antipolarized band will grow rapidly, abruptly transforming the system into the Hubbard's nonmagnetic state shown in Fig. 5.

For the purpose of simple illustration, we have discussed the nature of our solutions solely based on power expansions. In practice, the original cubic equations can be solved precisely without difficulties.

Finally, we shall discuss briefly the question of finding a ferromagnetic state instead of an antiferromagnetic state. The Hubbard Hamiltonian certainly admits a ferromagnetic solution. According to Herring,⁶ however, there is only fragmentary

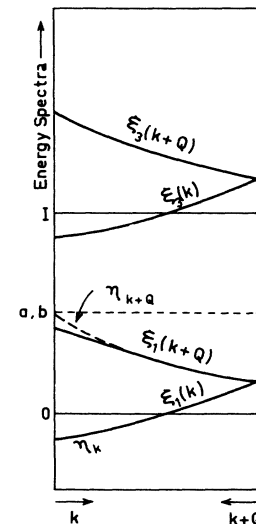


FIG. 5. Energy spectra for the nonmagnetic case ($M = 0$).

evidence that the ground state of the Hubbard Hamiltonian can ever be ferromagnetic. For any spin state, there are many opportunities for hopping without having an extra pair of two electrons on the same atom. Since a nonmagnetic state has the possibility of lowering the energy by allowing an optimum number of doubly occupied atoms, while the fully ferromagnetic state has no such opportunity, it is very unlikely that the exact ground state is ferromagnetic.

In the case of a linear chain of atoms with the hopping matrix elements $\epsilon_{RR'}$ nonzero only for nearest neighbors, Lieb and Mattis¹⁰ have proved that the ground state is always a singlet or a doublet but never ferromagnetic. Hubbard⁹ has calculated the ferromagnetic instability of a nonmagnetic state and shown that such instability can occur only if the density of states at the Fermi level is much higher than the average over the band.

These results incline one to suggest that the present model can never be ferromagnetic and the present treatment on the stability of an antiferromagnetic state against a nonmagnetic state will be justified even though the ferromagnetic instability is not considered. Ferromagnetism is expected to appear if the degeneracy of d electrons is explicitly taken into account, and then it becomes necessary to investigate the ferromagnetic instability of an antiferromagnetic solution. However, the spin polarization of bands which yields the antiferromagnetic stability against a nonmagnetic state is different from the splitting of spin-up and spin-down bands which leads to the ferromagnetic stability against the same nonmagnetic state. The ferromagnetic instability of an antiferromagnetic solution is not known, and we have to compare the energies of the two-distinct state to see which one of the solutions is more stable than the other.

*Work performed under the auspices of the U. S. Atomic Energy Commission and the Consiglio Nazionale delle Ricerche, Italy.

†On leave of absence from Argonne National Laboratory during 1970–71.

¹D. Adler, in *Solid State Physics*, edited by F. Seitz, D. Turnbull, and H. Ehrenreich (Academic, New York, 1969), Vol. 21, p. 1.

²J. C. Slater, *Phys. Rev.* **82**, 538 (1951).

³J. Hubbard, *Proc. Roy. Soc. (London)* **A276**, 238 (1963).

⁴J. Hubbard, *Proc. Roy. Soc. (London)* **A281**, 401 (1964).

⁵D. N. Zubarev, *Usp. Fiz. Nauk* **71**, 71 (1960); [*Sov.*

Phys. Usp. **3**, 320 (1960)].

⁶C. Herring, in *Magnetism*, edited by G. T. Rado and H. Suhl (Academic, New York, 1966), Vol. IV, Chap. X.

⁷See, for instance, A. B. Harris and R. V. Lange, *Phys. Rev.* **157**, 295 (1967); D. M. Esterling and R. V. Lange, *Rev. Mod. Phys.* **40**, 796 (1968); D. M. Edwards and A. C. Hewson, *Rev. Mod. Phys.* **40**, 810 (1968).

⁸T. Matsubara and T. Yokota, in *Proceedings of the International Conference on Theoretical Physics, Kyoto and Tokyo, September, 1953* (Science Council of Japan, Tokyo, 1954), p. 693.

⁹J. des Cloizeaux, *J. Phys. Radium* **20**, 606 (1959); **20**, 751 (1959).

¹⁰E. Lieb and D. Mattis, *Phys. Rev.* **125**, 164 (1962).

General Theory of Magnetic Pseudopotentials

Narayan C. Das and Prasanta K. Misra*

Department of Physics, Utkal University, Bhubaneswar-4, Orissa, India

(Received 27 January 1971)

A general magnetic-pseudopotential theory has been developed for Bloch electrons in a magnetic field. This theory is a generalization of the earlier formulations of Misra and Roth, and Misra, and it includes the effects of spin and spin-orbit interaction. In this method, tight-binding and orthogonalized-plane-wave functions are constructed which have the symmetry of the magnetic Bloch functions and which form a complete set for the wave function of the Hamiltonian of the crystal in a magnetic field. These are used as basis states for the wave function of an eigenstate of the problem, and an effective Hamiltonian is obtained which includes the magnetic pseudopotential. The magnetic pseudopotentials due to Misra and Roth, and Misra, and zero-field pseudopotentials, are obtained from this general magnetic pseudopotential in appropriate limits. The expression for the magnetic pseudopotential has been obtained in a form such that it can be calculated to any order in the magnetic field. This expression is further simplified for metals. The immediate purpose of this formulation is to calculate the total magnetic susceptibility of metals and alloys.

I. INTRODUCTION

Recently, Misra and Roth¹ have introduced a

modified pseudopotential method in the theory of Bloch electrons of simple metals in a magnetic field. Misra² has extended this method, which he